

A novel peptide electrochemical biosensor for heparin based on the dual “turn-on” signals of Ag/2D CuTCPP(Fe)

Fan Zhao*, Jingyue Lan and Yunxi Liu

Tianjin Key Laboratory of Structure and Performance for Functional Molecules, College of Chemistry, Tianjin Normal University, Tianjin 300387, China

** Corresponding author.*

E-mail addresses: fzhao@tjnu.edu.cn

Experimental section

Reagents and Chemicals. The specific recognition peptide sequence (Pep, 2-Nal-RKRLQVQLSIRT, purity > 95%), biotin modified peptide (Biotin-Pep, Biotin-RKRLQVQLSIRT, purity > 95%) and fluorescein isothiocyanate-labeled peptide (FITC-Pep, FITC-KRKRLQVQLSIRT, purity > 95%) were synthesized by Suzhou Motif Biotech Co., Ltd. (Suzhou, China). Streptavidin modified magnetic beads (SAM-B) were bought from BioCanal Scientific Inc. (Shanghai, China). Materials for the synthesis of 2D CuTCPP(Fe) including $\text{Cu}(\text{NO}_3)_2 \cdot 3\text{H}_2\text{O}$, trifluoroacetic acid (TFA), Fe(III) tetra(4-carboxyphenyl)porphine chloride (TCPP(Fe)), polyvinylpyrrolidone (PVP, MW=40000 g/mol), ethanol (EtOH) and N,N-dimethylformamide (DMF) were delivered by Bidepharm Technology Co., Ltd. (Shanghai, China). The synthesis of Ag nanoparticles employed AgNO_3 and NaBH_4 were obtained from Macklin Biochemical Technology Co., Ltd. (Shanghai, China). Bovine serum albumin (BSA), glucose, uric acid (UA), ascorbic acid (AA), 1,2-diaminobenzene (*o*-PD), 30% H_2O_2 and 1,4-dicarboxybenzene (TA) were offered by Meryer Chemical Technology Co., Ltd. (Shanghai China). KCl and ferricyanide including $\text{K}_4[\text{Fe}(\text{CN})_6]$ and $\text{K}_3[\text{Fe}(\text{CN})_6]$ were purchased from Chron Chemicals Co., Ltd. (Chengdu, China). Carbon nanotubes (CNTs) were got from Jiangsu XFNANO Materials Technology Co., Ltd. (Nanjing, China). Heparin sodium salt (Hep), chondroitin sulfate sodium (ChS), hyaluronic acid sodium (HA), adenosine-5'-diphosphate disodium salt (ADP), adenosine-5'-monophosphate disodium salt (AMP) and adenosine-5'-triphosphate disodium salt hydrate (ATP) were received from Beijing Solarbio Science & Technology Co., Ltd. (Beijing, China). The supporting electrolyte was phosphate buffer solution (PBS, 0.1 M, pH 7.4). The materials utilized in this study were commercially available and were not subjected to further purification.

Apparatus and Measurements. Transmission electron microscopy (TEM) and energy dispersive spectrometry (EDS) mapping were obtained from Talos F200X (Czech Republic). X-ray photoelectron spectroscopy (XPS) was conducted on Kratos AXIS ULTRA^{DL}D (Japan). Fluorescence spectroscopy measurements were executed on Agilent Cary Eclipse. The crystal structures of 2D CuTCPP(Fe) and Ag/2D CuTCPP(Fe) were investigated using X-ray diffraction (XRD, Bruker D8 ADVANCE). Electrochemical measurements of cyclic voltammetry (CV), differential pulse voltammetry (DPV) and electrochemical impedance spectroscopy (EIS) were carried out using a CHI 760E electrochemical workstation (Chenhua, Shanghai, China). A three-electrode structure was employed with the working electrode of glassy carbon electrode (GCE), the reference electrode of Ag/AgCl electrode, and the counter electrode of platinum wire (Pt).

Preparation of 2D CuTCPP(Fe) and Ag/2D CuTCPP(Fe) nanosheets. Initially, Cu(NO₃)₂·3H₂O (2.4 mg), TFA (40 μL, 1.0 M), and PVP (10 mg) were dispersed in a mixed solvent (12 mL, V_{DMF} : V_{EtOH} = 3:1). Then dissolved TCPP(Fe) (4.0 mg in 4 mL solvent mixture, V_{DMF} : V_{EtOH} = 3:1) was added drop-wise under stirring. After stirring for 10 min, the solution was placed into a reactor and kept at 80 °C for 4 h. Let the reactor cool to ambient temperature, and the resultants were got by centrifugation with subsequent rinse using EtOH. Finally, the 2D CuTCPP(Fe) nanosheets were obtained via drying overnight.

Ag/2D CuTCPP(Fe) nanomaterials were synthesized through the direct reduction of AgNO₃ using NaBH₄ on the 2D CuTCPP(Fe) surface. Firstly, 2D CuTCPP(Fe) (10 mg) was completely distributed in 20 mL of distilled water. Then AgNO₃ solution (2.0 mM, 2 mL) was added, which was mixed thoroughly by sonication. Thereafter, 1.5 mL of freshly prepared NaBH₄ solution (10.0 mM) was introduced drop-wise under intense stirring. The mixture was kept stirring for 2 h, followed by centrifugation and washing with EtOH, and then dried to yield Ag/2D CuTCPP(Fe) nanocomposites.

Preparation of Pep/Ag/2D CuTCPP(Fe) labels. In a typical procedure, 3.0 mg of Ag/2D CuTCPP(Fe) nanomaterials were dispersed in 1.0 mL PBS solution (0.1 M, pH 7.4) containing 20 μg/mL Pep. The resulting solution was sonicated for 15 s and incubated overnight at 4 °C to ensure that the peptides were firmly anchored to the surface of the nanomaterials via π-π stacking. After centrifugation and purification, the prepared Pep/Ag/2D CuTCPP(Fe) labels were re-dispersed in PBS solution (0.1 M, pH 7.4) and stored at 4 °C for further experiments.

Construction of the electrochemical sensing platform. The “turn-on” electrochemical biosensor with dual-signal output was constructed as follows. GCE with a diameter of 3 mm was cleaned first using 0.05 μm Al_2O_3 polishing powder, then rinsed thoroughly with distilled water and EtOH to obtain a smooth surface. 4 μL of CNTs dispersion (2.0 mg/mL, DMF) was dripped on the electrode and dried under a heat lamp to acquire GCE/CNTs sensing matrix. Then, Pep (20 $\mu\text{g}/\text{mL}$) was assembled on the electrode at 4 $^\circ\text{C}$ for 12 h via π - π stacking between naphthalene and CNTs. The unbonded Pep was washed with PBS buffer to afford GCE/CNTs/Pep electrode. Subsequently, BSA (3 μL , 1 wt%) was utilized for blocking non-specific binding sites, resulting in GCE/CNTs/Pep/BSA electrode. The above modified electrode was incubated in a range of Hep standard solutions with varied concentrations, respectively, for 40 min to obtain GCE/CNTs/Pep/BSA/Hep. Finally, the prepared Pep/Ag/2D CuTCPP(Fe) labels (3.0 mg/mL) were dropped on the electrode to make them firmly bonded to the Hep through electrostatic interaction. The loosely bound labels were removed with PBS buffer. And the resulting sensing platform was denoted as GCE/CNTs/Pep/BSA/Hep/Pep/Ag/2D CuTCPP(Fe). To maintain activity, the electrodes were stored at 4 $^\circ\text{C}$ prior to use.

The modification process of the dual-signal biosensor was characterized by CV and EIS in 5 mM $\text{Fe}(\text{CN})_6^{3-/4-}$ with 0.1 M KCl. CV was performed within $-0.2 \sim 0.6$ V at 0.1 V/s. The settings for EIS were as follows: initial potential of open circuit potential, amplitude of 0.005 V, and frequency range of 0.1-10⁵ Hz. Electrochemical detection of Hep was performed using DPV with parameters as 4 mV of increment potential, 0.05 V of amplitude, 0.06 s of pulse width, and 0.5 s of pulse period. The solid-state Ag/AgCl signal was recorded in PBS buffer with the optimal Cl^- concentration for the quantification of Hep. Besides, the developed biosensor was also evaluated in N_2 -saturated PBS buffer with 10 mM *o*-PD and H_2O_2 to acquire the reduced signal of *o*-PD_{ox} as the second signal for Hep determination.

Monitoring of Hep metabolism in rat serum. All animal procedures were in accordance with the guide for the care and use of laboratory animals from Chinese Ministry of Health and approved by the Animal Ethics Committee of Tianjin Normal University (HX-2020-02). Male Wistar rats (250–300 g) were used in our experiments. Surgical procedures were carried out as previously reported.¹ 2 mL Hep saline solution (0.9%) with a concentration of 100 $\mu\text{g}/\text{mL}$ was administered intraperitoneally. 0.5 mL of blood was taken from the abdominal aorta of the rats at different time points (0.5, 1, 2, 3, 4, and 5 h) after dosing. Then blood samples were subjected to centrifugation at 3000 rpm for 15 min. The resulting supernatant was diluted 4-fold with 0.1 M PBS solution containing Cl^- to adjust Cl^- with the optimal concentration for electrochemical

detection. Throughout the surgical procedure, a heating pad was utilized to maintain the animals' body temperature at 37 °C.

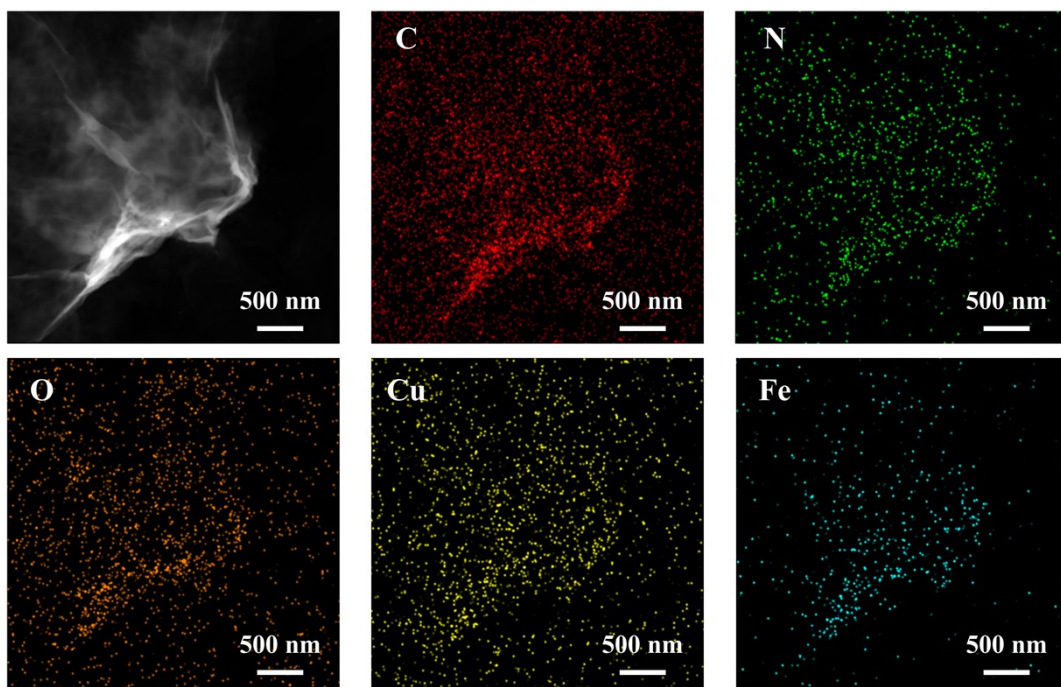


Fig. S1. Elemental mapping analysis of 2D CuTCPP(Fe).

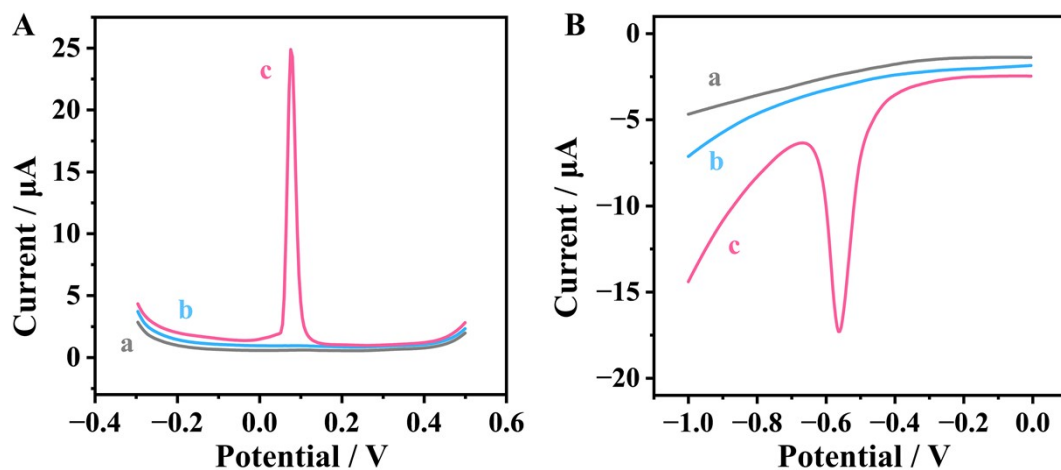


Fig. S2. (A) DPVs of GCE (a), GCE/CNTs (b), and GCE/CNTs/Ag/2D CuTCPP(Fe) (c) in 0.1 M PBS (pH 7.4) containing 60 mM Cl⁻. (B) DPVs of GCE (a), GCE/CNTs (b), and GCE/CNTs/Ag/2D CuTCPP(Fe) (c) in 0.1 M PBS (pH 7.4) containing 10 mM *o*-PD and 10 mM H₂O₂.

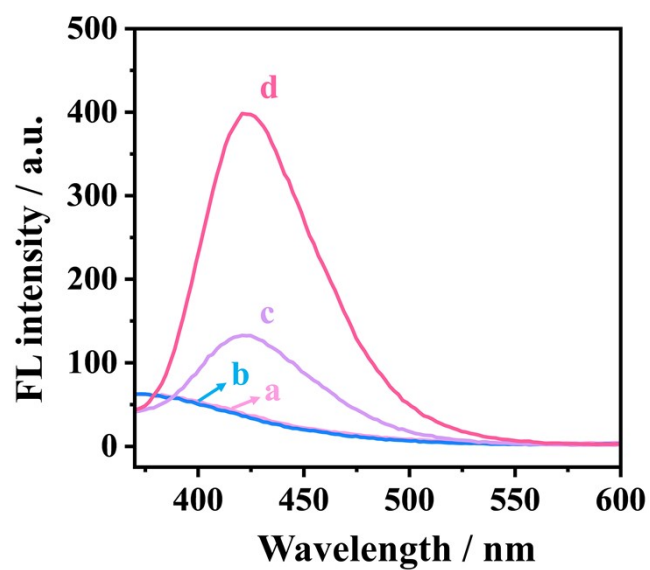


Fig. S3. Fluorescence emission spectra of 0.5 mM TA (a), 0.5 mM TA+1.0 mg/mL Ag/2D CuTCPP(Fe) (b), 0.5 mM TA+500 mM H₂O₂ (c), and 0.5 mM TA+500 mM H₂O₂+1.0 mg/mL Ag/2D CuTCPP(Fe) (d).

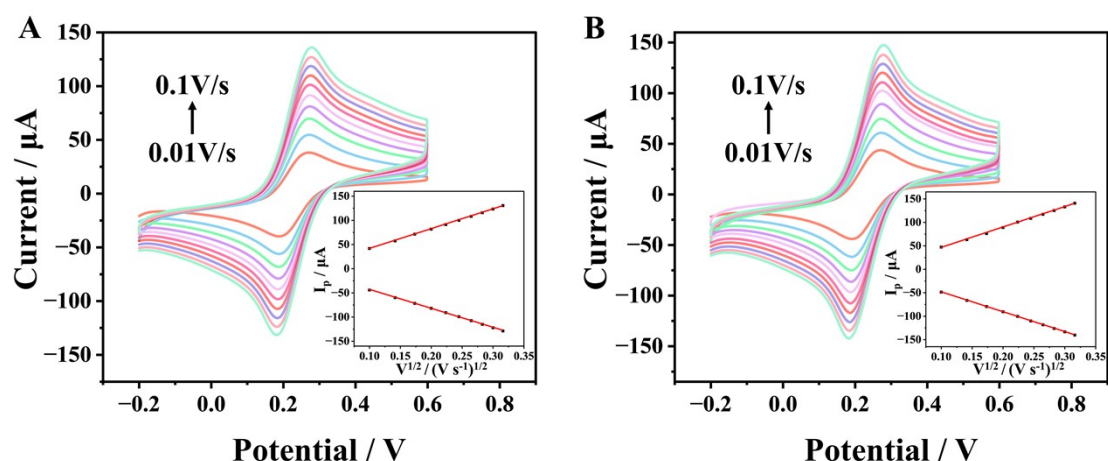


Fig. S4. CV curves obtained at (A) GCE/CNTs and (B) GCE/CNTs/Ag/2D CuT CPP(Fe) modified electrodes at varying scan rates from 0.01 V s⁻¹ to 0.1V s⁻¹ in 5 mM Fe(CN)₆^{3-/4-} containing 0.1 M KCl.

The electroactive surface of modified electrodes was assessed through CV experiments. The peak current (I_p) increased gradually as the increasing scan rates, and exhibited a good linear correlation with the square root of the scan rate ($v^{1/2}$). This observation indicated that the redox reaction at the electrode is a diffusion-controlled process. Based on the Randles-Sevcik equation, the effective electroactive areas of CNTs and CNTs/Ag/2D CuT CPP(Fe) were determined to be 0.1177 cm² and 0.1251 cm², respectively, compared to bare GCE electrode (0.071cm²). This confirmed the effectiveness of the amplification effect of CNTs matrix and Ag/2D CuT CPP(Fe), which would inevitably deliver a good current response.

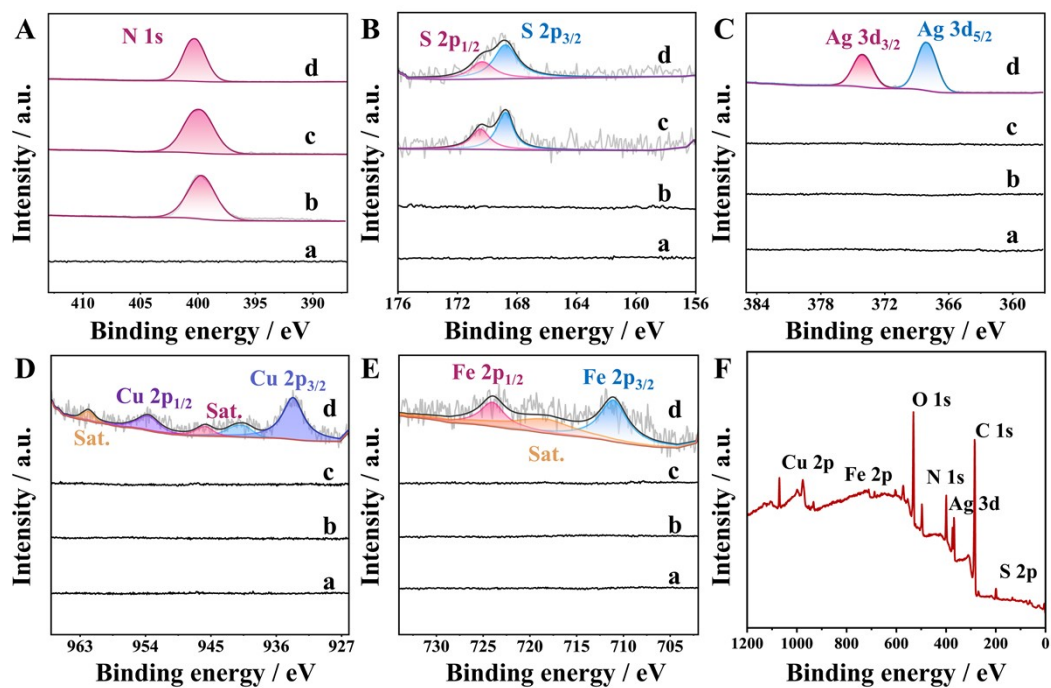


Fig. S5. XPS spectra of (A) N 1s, (B) S 2p, (C) Ag 3d, (D) Cu 2p, and (E) Fe 2p for GCE/CNTs (a), GCE/CNTs/Pep (b), GCE/CNTs/Pep/Hep (c), and GCE/CNTs/Pep/Hep/Pep/Ag/2D CuTCPP(Fe) (d). (F) XPS survey spectrum of GCE/CNTs/Pep/Hep/Pep/Ag/2D CuTCPP(Fe).

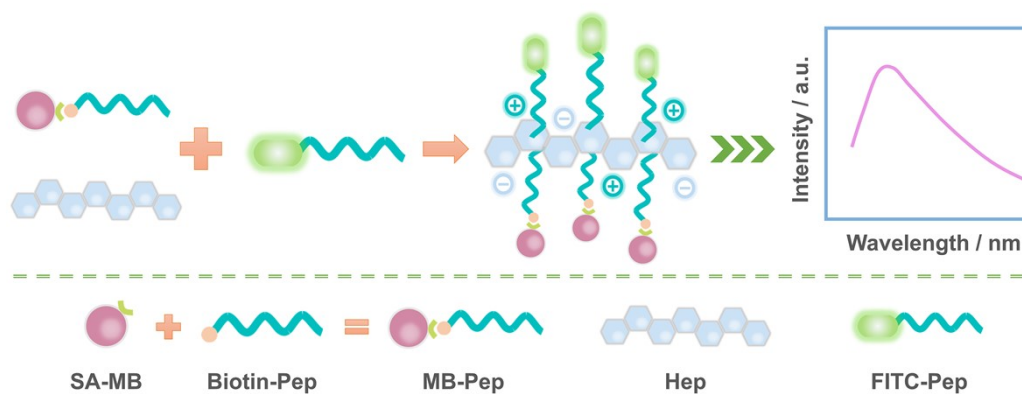


Fig. S6. Schematic illustration of the protocol for validation of the Pep recognition with Hep by fluorescence analysis.

To further verify the feasibility of our strategy, fluorescence tests were carried out. As shown in Figure S6, two kinds of peptides were designed. One was magnetic beads modified peptide (MB-Pep) combined through biotin-streptavidin. The other one was fluorescein isothiocyanate-labeled peptide (FITC-Pep). FITC-Pep and MB-Pep were incubated with Hep at room temperature for 40 min. After magnetic separation to remove the excess reagents, fluorescence tests were conducted. As shown in Figure S7, there were no signal for MB-Pep and MB-Pep + Hep system. Whereas, a pronounced signal appeared at 520 nm for MB-Pep + Hep + FITC-Pep system, thus proving the feasibility of the recognition strategy.

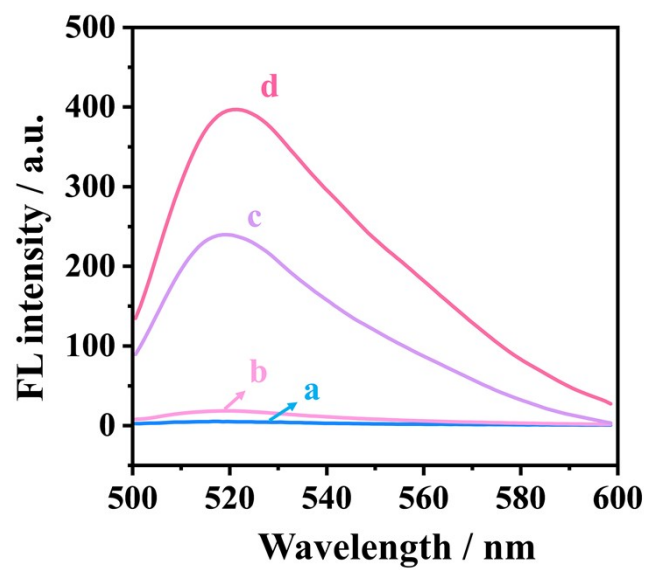


Fig. S7. Fluorescence tests of 10 $\mu\text{g}/\text{mL}$ MB-Pep (a), 10 $\mu\text{g}/\text{mL}$ MB-Pep + 10 $\mu\text{g}/\text{mL}$ Hep (b), 10 $\mu\text{g}/\text{mL}$ MB-Pep + 10 $\mu\text{g}/\text{mL}$ Hep + 10 $\mu\text{g}/\text{mL}$ FITC-Pep (c) and 10 $\mu\text{g}/\text{mL}$ MB-Pep + 20 $\mu\text{g}/\text{mL}$ Hep + 10 $\mu\text{g}/\text{mL}$ FITC-Pep (d).

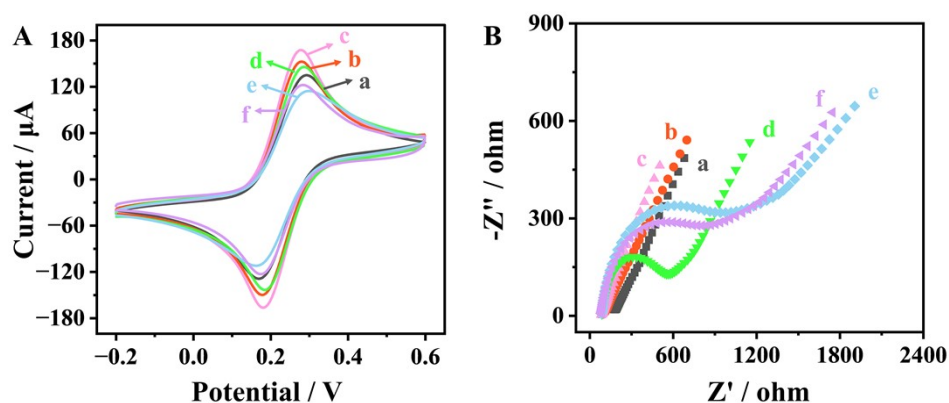


Fig. S8. (A) CV and (B) EIS of bare GCE (a), GCE/CNTs (b), GCE/CNTs/Pep (c), GCE/CNTs/Pep/BSA (d), GCE/CNTs/Pep/BSA/Hep (e), and GCE/CNTs/Pep/BSA/Hep/Pep/Ag/2D CuTCPP(Fe) (f) in 5 mM $\text{Fe}(\text{CN})_6^{3-/4-}$ containing 0.1 M KCl.

CV and EIS analysis were carried out to track the step-by-step modification process of the dual signal electrochemical biosensor. The bare GCE exhibited a pair of standard reversible redox peaks (Fig. S8A, curve a). Upon the modification of CNTs, the redox peak current increased significantly as a result of the enhanced electron transfer (Fig. S8A, curve b). Following the immobilization of the positively charged Pep, the redox current continued to increase under the influence of electrostatic interactions (Fig. S8A, curve c). Subsequently, the redox peak current declined gradually with the modification of BSA and Hep (Fig. S8A, curve d and e), which was attributed to the negative effect of biomolecules and electrostatic repulsion on the electron transfer. With the further interaction with Pep/Ag/2D CuTCPP(Fe), a slight increase in the peak current was observed due to the good electrical conductivity of Ag/2D CuTCPP(Fe) (Fig. S8A, curve f). Meanwhile, EIS curves were also monitored. The diameter of the semicircle in the Nyquist plot denotes the charge transfer resistance (R_{ct}). The bare GCE, GCE/CNTs and GCE/CNTs/Pep electrode showed small R_{ct} semicircles (Fig. S8B, curve a, b, and c). While the diameters of the semicircles increased gradually with the modification of BSA and Hep (Fig. S8B, curve d and e), and then decreased a little upon Pep/Ag/2D CuTCPP(Fe) assembly (Fig. S8B, curve f), which were in line with the CV results. The CV and EIS outcomes verified the successful modification processes of the dual signal electrochemical biosensor.

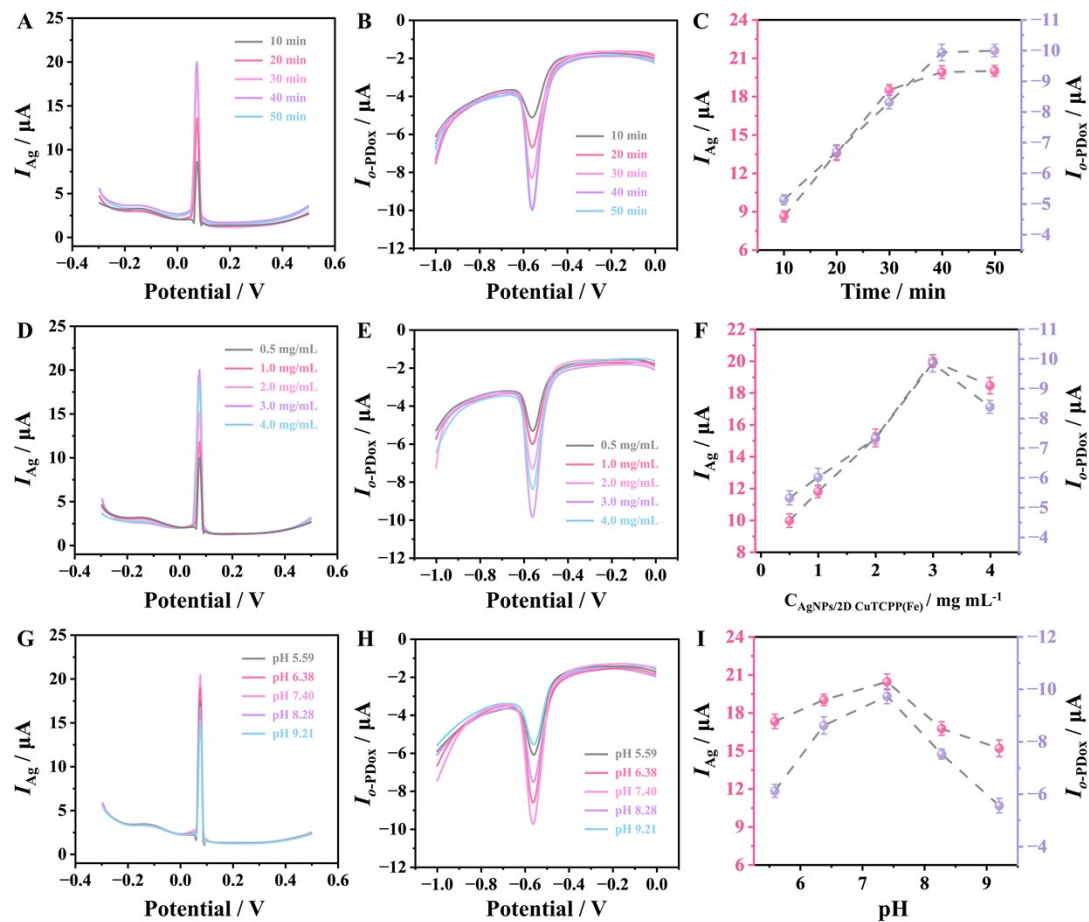


Fig. S9. Effects of (A, B and C) incubation time of Hep, (D, E and F) concentration of Ag/2D CuTCPP(Fe), and (G, H and I) pH value of PBS buffer on the DPV responses of the dual-signal output biosensor.

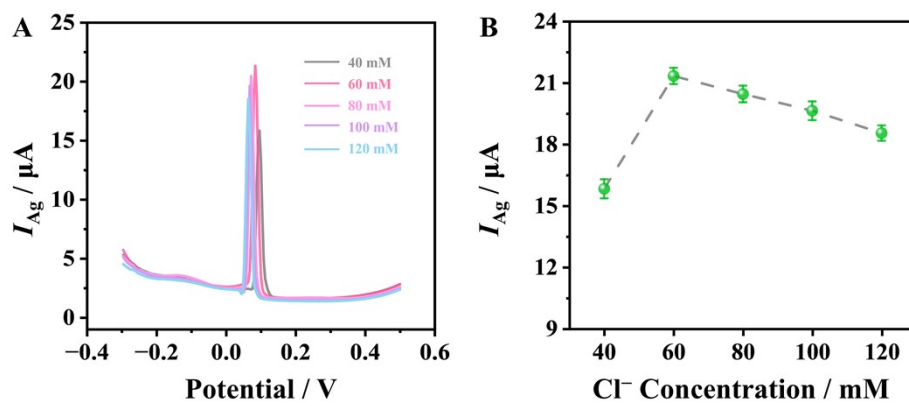


Fig. S10. Effect of Cl^- concentration on the solid-state Ag/AgCl response.

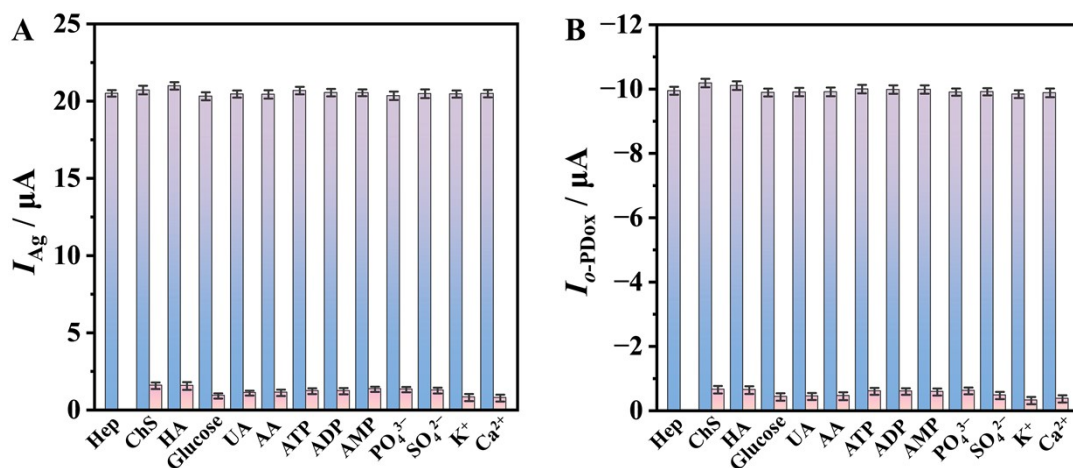


Fig. S11. Selectivity and competition test of the dual-signal electrochemical biosensor for Hep. (A) Peak current of I_{Ag} acquired at the present biosensor in 0.1 M PBS (pH 7.4) with 60 mM Cl^- towards 500 ng/mL Hep and associated interfering substances. (B) Peak current of I_{o-PDox} acquired at the present biosensor in 0.1 M PBS (pH 7.4) containing 10 mM *o*-PD and 10 mM H_2O_2 towards 100 ng/mL Hep and associated interfering substances. The concentrations of ChS and HA were added in the same amount as the Hep concentration, with the remaining interferences as follows: glucose of 1 mM, UA of 10 μM, AA of 10 μM, ATP of 10 μM, ADP of 10 μM, AMP of 10 μM, PO_4^{3-} of 1 mM, SO_4^{2-} of 1 mM, K^+ of 5 mM, and Ca^{2+} of 1 mM.

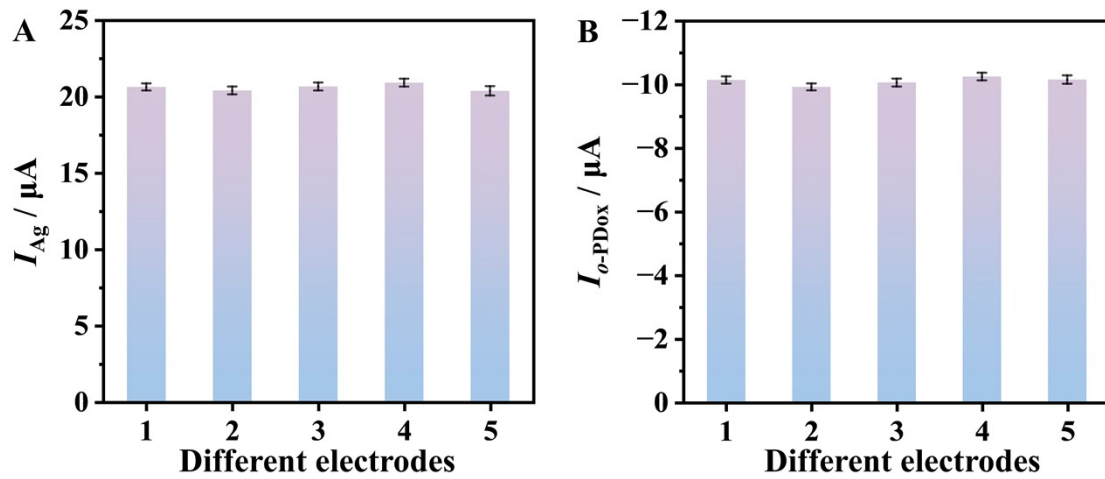


Fig. S12. Reproducibility tests for the present dual-signal electrochemical biosensor. (A) Peak current of I_{Ag} obtained from different electrodes in 0.1 M PBS (pH 7.4) containing 60 mM Cl^- for 500 ng/mL Hep. (B) Peak current of I_{o-PDox} obtained from different electrodes in 0.1 M PBS (pH 7.4) containing 10 mM *o*-PD and 10 mM H_2O_2 for 100 ng/mL Hep.

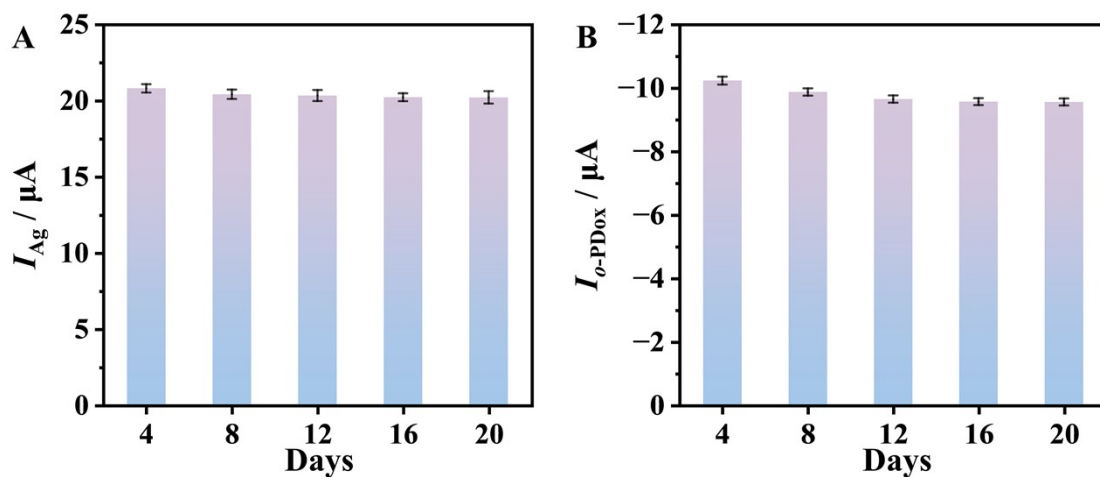


Fig. S13. Stability tests for the present dual-signal electrochemical biosensor. (A) Peak current of I_{Ag} obtained from the same electrode in 0.1 M PBS (pH 7.4) containing 60 mM Cl^- for 500 ng/mL Hep over 20 days. (B) Peak current of I_{o-PDox} acquired from the same electrode in 0.1 M PBS (pH 7.4) containing 10 mM *o*-PD and 10 mM H_2O_2 for 100 ng/mL Hep over 20 days.

Table S1. Comparison of different electrochemical sensors for Hep.

Electrochemical sensors	Linear range	LOD	Reference
MB-hep/Au	0.666 – 64.5 $\mu\text{g/mL}$	270 ng/mL	2
A poly(thionine) modified electrode	4.0 – 22.0 $\mu\text{g/mL}$	0.28 $\mu\text{g/mL}$	3
A polymeric membrane ion-selective electrode	0.025 – 0.984 $\mu\text{g/mL}$	0.012 $\mu\text{g/mL}$	4
$\text{Fe}(\text{CN})_6^{3-/4-}/\text{polyA}_2\text{-MWCNTs/Pt}$	0.615 – 49.2 $\mu\text{g/mL}$	0.615 $\mu\text{g/mL}$	5
GO/Au-protamine/GCE	9.22 ng/mL – 1.17 $\mu\text{g/mL}$	5.54 ng/mL	6
A two-zone of Graphene modified Carbon sensor	0.246 – 12.3 $\mu\text{g/mL}$	0.246 $\mu\text{g/mL}$	7
The present dual-signal output biosensor	0.01 ng/mL – 10 $\mu\text{g/mL}$	7.92×10^{-3} $\mu\text{g/mL}$ 8.43×10^{-3} $\mu\text{g/mL}$	This work

Table S2. Quantification of Hep in serum samples by the present electrochemical biosensor with dual-signal output (n=3).

Signal	Initial (ng/mL)	Added (ng/mL)	Found (ng/mL)	Recovery (%)	RSD (%)
Ag/AgCl signal	ND ^a	0.50	0.49	98.7	3.1
		1.00	1.01	101.3	2.1
		10.00	10.32	103.2	1.3
		20.00	20.19	100.9	0.8
<i>o</i> -PD _{ox} signal	ND ^a	0.50	0.48	96.0	2.1
		1.00	1.02	102.3	3.0
		10.00	10.02	100.2	0.8
		20.00	19.97	99.8	1.1

a: Not detected

Table S3. Determination of Hep in rat serum samples based on the present dual-signal biosensor.

Metabolic time	Ag/AgCl signal				o-PD _{ox} signal			
	Rat1	Rat2	Rat3	Mean±SD	Rat1	Rat2	Rat3	Mean±SD
	Hep (µg/mL)				Hep (µg/mL)			
0.5 h	7.58	6.45	5.38	6.47±1.10	7.69	5.31	6.27	6.42±1.20
3 h	1.47	1.11	1.01	1.20±0.24	1.43	1.10	0.91	1.15±0.26
5 h	0.53	0.18	0.17	0.29±0.21	0.45	0.31	0.09	0.28±0.18

A t test was made to determine whether the means obtained between the Ag/AgCl signal and o-PD_{ox} signal are distinct. The t value was calculated according to equation

$$t = \frac{|X_1 - X_2|}{s} \sqrt{\frac{n_1 n_2}{n_1 + n_2}} \quad (1)$$

in which $s = \sqrt{\frac{s_1^2(n_1 - 1) + s_2^2(n_2 - 1)}{(n_1 - 1) + (n_2 - 1)}}$, s_1 and s_2 represent the standard deviation of determined results by the Ag/AgCl signal and o-PD_{ox} signal, respectively. n_1 and n_2 are sample numbers of Ag/AgCl signal and o-PD_{ox} signal (herein, n_1 and n_2 is equal to 3). If the t value is larger than standard t value, 2.13 ($\alpha = 0.1$), the result obtained from Ag/AgCl signal was considered is not very consistent with that obtained from o-PD_{ox} signal.

Table S4. Determination of Hep in rat serum samples after drug metabolism for 3 h based on the dual-signal biosensor and the ELISA Kit.

Method	Rat1	Rat2	Rat3	Mean±SD
	Hep ($\mu\text{g/mL}$)			
Ag/AgCl signal	1.42	1.03	1.06	1.17±0.22
<i>o</i> -PD _{ox} signal	1.16	1.37	1.01	1.18±0.18
ELISA Kit	1.11	1.03	1.45	1.20±0.22

After the rats were intraperitoneally injected with 2 mL 100 $\mu\text{g/mL}$ Hep for 3 h, the Hep concentration in serum samples were determined by the present dual-signal output electrochemical biosensor and were compared with those obtained by the Hep ELISA Kit. The results were summarized in Table S4. According to the *t*-test ($\alpha=0.1$), no significant differences were observed between the developed electrochemical method and the commercial Hep assay kit ($t=0.15$ for Ag/AgCl signal and ELISA Kit; $t=0.10$ for *o*-PD_{ox} signal and ELISA Kit).

Reference

1. H. Qi, L. Zhang, L. Yang, P. Yu and L. Mao, *Anal. Chem.*, 2013, **85**, 3439-3445.
2. L. Tan, S. Yao and Q. Xie, *Talanta*, 2007, **71**, 827-832.
3. H. Y. Huo, H. Q. Luo and N. B. Li, *Microchim. Acta*, 2009, **167**, 195-199.
4. Y. Chen, R. N. Liang and W. Qin, *Chin. Chem. Lett.*, 2012, **23**, 233-236.
5. S.-N. Ding, J.-F. Chen, J. Xia, Y.-H. Wang and S. Cosnier, *Electrochem. Commun.*, 2013, **34**, 339-343.
6. A. Rengaraj, Y. Haldorai, S. K. Hwang, E. Lee, M.-H. Oh, T.-J. Jeon, Y.-K. Han and Y. S. Huh, *Bioelectrochemistry*, 2019, **128**, 211-217.
7. A. Zheng, W. Zhang, C. Li, Z. Guo, C. Li, C. Zhang, J. Yao, Z. Zhang, J. Li, S. Zhao and L. Zhou, *Biosens. Bioelectron.*, 2022, **198**, 113856.